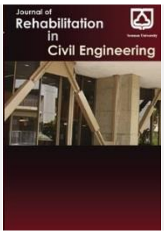

Journal of Rehabilitation in Civil Engineering

Journal homepage: https://civiljournal.semnan.ac.ir/

Performance Evaluation of Compressive Strength Models for SRP and SRG-Confined Concrete Columns

Ehsan Janfada [1]; HamidReza Nasseri [2]; Hashem Jahangir [2,*]

1. M.Sc. Student, Department of Civil Engineering, University of Birjand, Birjand, Iran
2. Detarrment of Civil Engineering, Research Group of Novel Technologies in Civil Engineering, University of Birjand, Birjand, Iran

* Corresponding author: *h.jahangir@birjand.ac.ir*

ARTICLE INFO

Article history:
Received: 22 May 2023
Revised: 03 July 2023
Accepted: 07 July 2023

Keywords:
Compressive strength models;
Performance evaluation;
SRP composites;
SRG composites;
Confined columns.

ABSTRACT

This paper focused on confining effects of externally bonded composites with polymer and grout matrices equipped with steel fibers, respectively named steel reinforced polymer (SRP) and steel reinforced grout (SRG) composites, as novel and effective methods of strengthening structures. To achieve this goal, an experimental database including 13 and 10 concrete columns with square cross-sections respectively confined by SRP and SRG composites was compiled from a recent empirical study. Moreover, after a comprehensive review and conducting a trial and error process of 45 existing models for estimating the relative compressive strength of confined concrete columns, six models for the SRP-confined concrete columns and six models for SRG-confined concrete columns with square cross-sections were selected and their performance was evaluated by comparing the Pearson correlation coefficient (R) and the mean absolute percentage error (MAPE) criteria. The results illustrated that for the SRP-confined concrete columns with square cross-sections, the selected model from the CNR-DT200 standard with respectively R and MAPE values of 0.7671 and 7.39% outperformed other selected SRP models. On the other hand. for the SRG-confined concrete columns with square cross-sections, the selected model from the research work of Isleem et al. with respectively R and MAPE values of 0.4405 and 18.45% surpassed the other selected SRP models. As most of the proposed models to estimate the relative compressive strength of confined concrete columns were suggested for the fiber-reinforced polymer (FRP) composites rather than the textile-reinforced mortar (TRM) composites, the overall comparison showed that all the selected SRP models outperformed the selected SRG models.

E-ISSN: 2345-4423

How to cite this article:
Janfada, E., Nasseri, H., & Jahangir, H. (2024). Performance Evaluation of Compressive Strength Models for SRP and SRG-Confined Concrete Columns. Journal of Rehabilitation in Civil Engineering, 12(2), 69-82. https://doi.org/10.22075/jrce.2023.30715.1855

1. Introduction

Concrete structures during their service life encounter various types of damage from natural and human hazards [1,2]. To avoid these damages, different strengthening techniques were introduced by the researchers [3,4]. One of the most regular strengthening methods is utilizing externally bonded composites [5].

Fiber-reinforced polymer (FRP) composites are one of the known externally bonded composites which were used to strengthen different concrete structural elements rely on their unique advantages such as high strength-to-weight values, and easy and rapid installation [6]. The polymer type of matrix used in FRP composite causes some drawbacks for utilizing the FRP composites in humid environments and makes the FRP composites sensitive to temperature. Therefore, researchers introduced textile-reinforced mortar (TRM) and fiber-reinforced grout (FRG) composites as an alternative to FRP composites in such environments [7–9].

The concrete columns, as essential structural elements, and specifically their strengthening techniques were the core focus of various research works [10,11]. The confining effects of FRP and TRM composites on concrete columns were studied in many previous publications [12–15]. Some research works were conducted to experimentally test the confined concrete columns with FRP and TRM composites [16–18]. In some other analytical studies, the confining influence of externally bonded FRP and TRM composites was estimated by providing predictive models [19–21]. Although, the number of proposed analytical models for estimating the compressive strength of TRM-confined concrete columns is much lower than that of FRP-confined concrete columns [22,23]. Moreover, the literature review showed that most of the studies concentrated on confined concrete columns with circular cross-sections, and the number of experimental and analytical research works designated to confined concrete columns with square and rectangular cross-sections are lower in comparison to circular concrete columns [24–28].

2. Research significance

The results of previous publications regarding the FRP and TRM-confined concrete columns showed that the following research gaps still exist and should be addressed in future research works:

- Although based on more consistency to stress distribution, the performance of concrete columns with circular cross-sections is better than that of concrete columns with square and rectangular cross-sections, as a result of easier construction, the concrete columns with square and rectangular cross-sections are more regular and should be in the core of focus in research works.
- Most of the present models for estimating the compressive strength of confined concrete columns were designated to FRP-confined concrete columns and fewer models were provided to estimate the compressive strength of TRM-confined concrete columns.
- Most of the utilized fibers in external composites are carbon, glass, aramid, and basalt and fewer studies concentrated on novel steel fibers in FRP and TRM composites.

In this paper, an effort has been conducted to concentrate on concrete columns with square cross-sections which are confined by both SRP and SRG composites, in which the novel steel fibers were utilized as the fiber layer. A comprehensive investigation was conducted to compile existing models for estimating the relative compressive strength of SRP and SRG-confined concrete columns and by doing the performance evaluation process, the best models were selected by applying them to a new experimental database.

3. Experimental database

To evaluate the existing models for estimating the compressive strength of confined concrete columns, in this paper, an experimental database was compiled from a recent study conducted by Jahangir et al. [29] which tested 13 SRP-confined and 10 SRG-confined concrete columns with square cross-sections. As illustrated in Fig. 1, they considered the width, length, and radius of the corner of the cross-section of the concrete columns, respectively denoted by *a*, *b,* and *r*, as geometrical influential input parameters. Moreover, the tensile strength, elastic modulus, thickness, and the number of layers of utilized steel fibers, respectively named f_f, E_f, t_f, and n_f, as well as the compressive strength of unconfined concrete column (f_{co}), were considered as mechanical influential input parameters affected the relative compressive strength of confined concrete columns (f_{cc}/f_{co}) as the sole output parameter. Table 1 reported the values of inputs and output parameters in the selected experimental database. Furthermore, Fig. 2 demonstrated the scattered diagrams of each input parameter vs. the output.

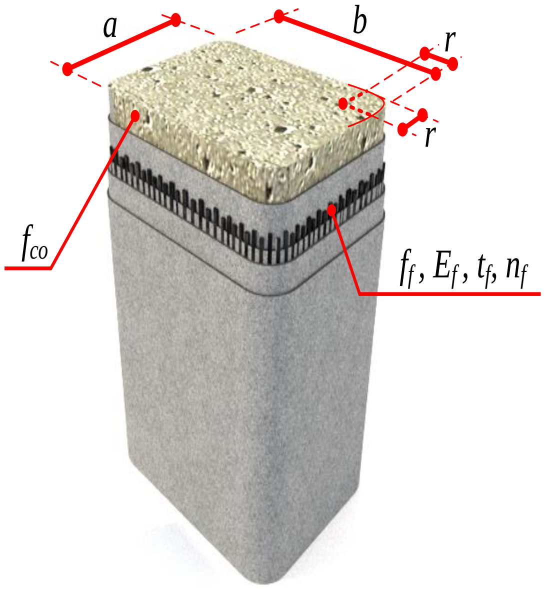

Fig. 1. The influential input parameters on compressive strength of confined concrete columns.

4. Selected existing models

In this paper, among the 45 existing models for estimating the relative compressive strength of confined concrete columns with square and rectangular by external composites presented in the study of Pimanmas and Saleem [30], the best 6 models, for each set of experimental data including SRP and SRG-confined concrete columns, respectively named SRP_M1 to SRP_M6 and SRG_M1 to SRG_M6, were selected to be presented and evaluated. The initial evaluation showed that 4 existing models were similar among the selected 6 models for SRP and SRG-confined concrete columns. As a result, in total, 8 existing models, named R1 to R8, were evaluated in the current study. Table 2 reported the overall selected R1 to R8 existing models and Table 3 classified them into SRP_M1 to SRP_M6 and SRG_M1 to SRG_M6 models.

Table 1. The compiled experimental database [29].

Confinement Composite	Specimen No.	Inputs								Output
		a (mm)	b (mm)	r (mm)	f_f (Mpa)	E_f (Gpa)	t_f (mm)	n_f	f_{co} (Mpa)	f_{cc}/f_{co}
SRP	1	150	150	17.5	3100	192	0.254	1	25.95	1.35
	2	150	150	17.5	3100	192	0.254	1	25.95	1.38
	3	150	150	17.5	3100	192	0.254	1	25.95	1.44
	4	150	150	0	3100	192	0.254	1	25.95	1.47
	5	150	150	0	3100	192	0.254	1	25.95	1.53
	6	150	150	0	3100	192	0.254	1	25.95	1.49
	7	150	150	0	3100	192	0.254	1	25.95	1.51
	8	150	150	17.5	3100	192	0.254	1	25.95	1.44
	9	150	150	17.5	3100	192	0.254	1	25.95	1.46
	10	150	150	17.5	3100	192	0.254	1	25.95	1.47
	11	150	150	17.5	3100	192	0.169	1	25.95	1.41
	12	150	150	17.5	3100	192	0.169	1	25.95	1.37
	13	150	150	17.5	3100	192	0.169	1	25.95	1.41
SRG	1	150	150	0	3100	192	0.254	1	25.95	1.15
	2	150	150	0	3100	192	0.254	1	25.95	1.28
	3	150	150	0	3100	192	0.254	1	25.95	1.16
	4	150	150	17.5	3100	192	0.254	1	25.95	1.14
	5	150	150	17.5	3100	192	0.254	1	25.95	1.17
	6	150	150	17.5	3100	192	0.254	2	25.95	1.37
	7	150	150	17.5	3100	192	0.254	2	25.95	1.30
	8	150	150	0	3100	192	0.169	1	25.95	1.29
	9	150	150	0	3100	192	0.169	1	25.95	1.34
	10	150	150	0	3100	192	0.169	1	25.95	1.30

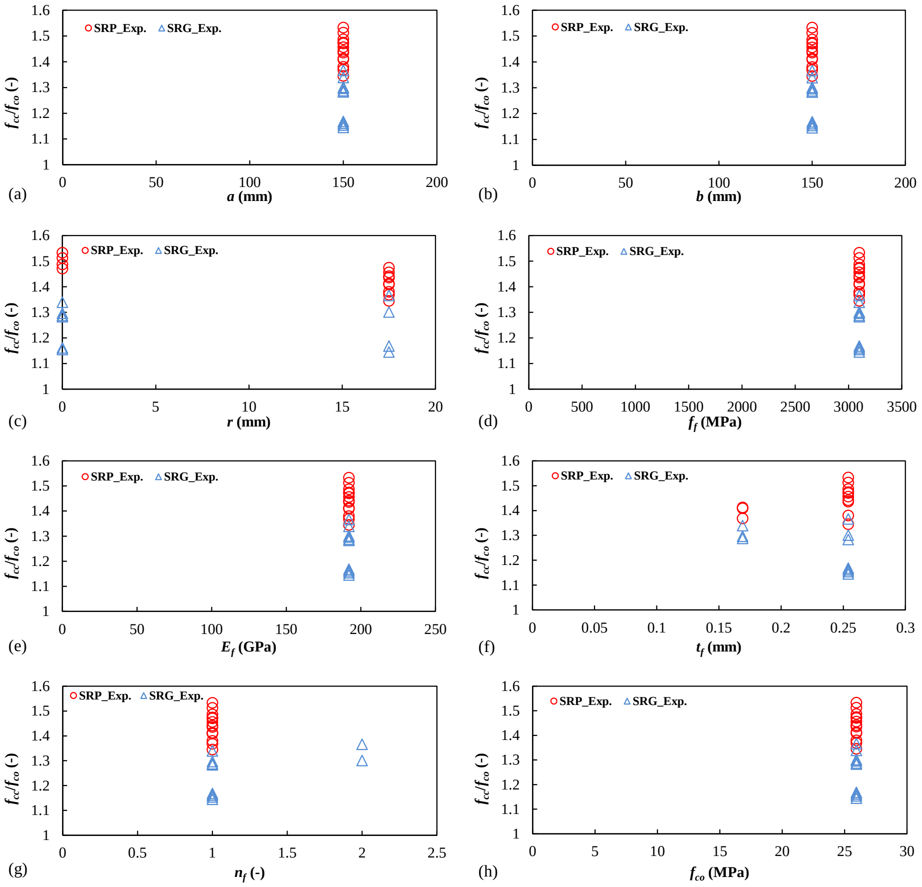

Fig. 2. The scattered diagrams of each input parameter vs. the output.: a) a; b) b; c) r; d) f_f; e) E_f; f) t_f; g) n_f and h) f_{co}.

Table 2. The overall selected existing models.

Reference	Model	Reference	Model
CNR-DT200 [31] – R1	$\frac{f_{cc}}{f_{co}} = 1.0 + 2.6\left(\frac{f_{l,e}}{f_{co}}\right)^{2/3}$ $f_{l,e} = k_e f_l;\ f_l = \frac{1}{2}\rho_f E_f \varepsilon_f$ $k_e = k_H k_v k_\alpha$ $\rho_f = \frac{4n_f t_f (a+b)}{b-a}$ $k_\alpha = \frac{1}{1+\tan^2\alpha}$ $k_H = 1 - \frac{a'^2 + b'^2}{3A_g};$ $a' = a - 2r;\ b' = b - 2r$ $A_g = ab - (4-\pi)r^2$ α: Angle of fibers with cross-section surface For continuous jackets with fibers: $k_v = 1$	Colajanni et al. [32] – R2	$\frac{f_{cc}}{f_{co}} = 2.254\sqrt{1 + 7.94\frac{f_{l,e}}{f_{co}}} - 2\frac{f_{l,e}}{f_{co}} - 1.254$ $f_{l,e} = k_e f_l;\ f_l = \frac{1}{2}\rho_f E_f \varepsilon_f$ $k_e = 1 - \frac{a'^2 + b'^2}{3A_g}$ $\rho_f = \frac{4n_f t_f}{D}$ $D = \sqrt{a^2 + b^2}$
Frangou et al. [33] – R3	$\frac{f_{cc}}{f_{co}} = 1.125 + 1.25\alpha\omega_w;\ \alpha\omega_w \geq 0.1$ $\frac{f_{cc}}{f_{co}} = 1 + 2.5\alpha\omega_w;\ \alpha\omega_w \leq 0.1$ $\omega_w = \frac{(2a+2b)}{t_f f_f ab f_{co}}, \alpha = \frac{A_e}{A_c}$ $A_c = ab,\ A_e = ab - 2\left(\frac{a^2}{6} - \frac{b^2}{6}\right)$	Hoshikuma et al. [34] – R4	$\frac{f_{cc}}{f_{co}} = 1.0 + 0.73\left(\frac{f_l}{f_{co}}\right)$ $f_l = \frac{1}{2}\rho_f E_f \varepsilon_f$
Thériault and Neale [35] – R5	$\frac{f_{cc}}{f_{co}} = 1.0 + \left(\frac{f_l}{f_{co}}\right)$ $f_l = \frac{2n_f t_f E_f \varepsilon_f (a+b)}{ab}$ $\varepsilon_f = \frac{f_f}{E_f}$	Kumutha et al. [36] – R6	$\frac{f_{cc}}{f_{co}} = 1.0 + 0.93\left(\frac{f_l}{f_{co}}\right)$ $f_l = \frac{1}{2}\rho_f f_f$ $\rho_f = \frac{2(a+b)n_f t_f}{ab}$
Islam et al. [37] – R7	$\frac{f_{cc}}{f_{co}} = 1.0 + 2.35\left(\frac{f_l}{f_{co}}\right)$ $f_l = \frac{2E_f \varepsilon_f n_f t_f}{D}$ $D = \sqrt{a^2 + b^2}$	Isleem et al. [38] – R8	$\frac{f_{cc}}{f_{co}} = 1 + 0.07\left(\frac{b}{a}\right)^{2.86}\left(\frac{f_{l,e}}{f_{co}}\right)^{2.64}$ $f_{l,e} = k_e \rho_f f_f;\ \rho_f = \frac{4n_f t_f}{D};\ k_e = \frac{A_{cf}}{A_g}$ $A_{cf} = A_g - \frac{(a-2r)^2 + (b-2r)^2}{3}$ for $\frac{(b-2r)^2}{4} \leq \frac{a}{2}$ $A_{cf} = A_g - \frac{(a-2r)^2 + (b-2r)^2}{3} + \frac{4}{3}h_0\sqrt{\frac{(b-2r)h_0}{2}}$ for $\frac{(b-2r)^2}{4} \geq \frac{a}{2}$ $h_0 = 2\left(\frac{(b-2r)}{4} - \frac{a}{2}\right)$ $D = \frac{2ab}{(a+b)}$

Table 3. Designated existing models to related SRP and SRG models.

Confinement Composite	Model	Designated Existing Model
SRP	SRP_M1	CNR-DT200 [31] – R1
	SRP_M2	Colajanni et al. [32] – R2
	SRP_M3	Frangou et al. [33] – R3
	SRP_M4	Thériault and Neale [35] – R5
	SRP_M5	Kumutha et al. [36] – R6
	SRP_M6	Hoshikuma et al. [34] – R4
SRG	SRG_M1	Isleem et al. [38] – R8
	SRG_M2	Islam et al. [37] – R7
	SRG_M3	Hoshikuma et al. [34] – R4
	SRG_M4	Kumutha et al. [36] – R6
	SRG_M5	Thériault and Neale [35] – R5
	SRG_M6	Frangou et al. [33] – R3

5. Performance evaluation

To evaluate the performance of designated models named SRP_M1 to SRP_M6 and SRG_M1 to SRP_M6, presented in Table 3, the Pearson correlation coefficient (R) and the mean absolute percentage error (MAPE) criteria were calculated in this paper based on the following equations:

$$R = \frac{\sum_{i=1}^{N}\left(\left(\frac{f_{cc}}{f_{co}}\right)_i - \overline{\left(\frac{f_{cc}}{f_{co}}\right)}\right)\left(\widetilde{\left(\frac{f_{cc}}{f_{co}}\right)}_i - \overline{\widetilde{\left(\frac{f_{cc}}{f_{co}}\right)}}\right)}{\sqrt{\sum_{i=1}^{N}\left(\left(\frac{f_{cc}}{f_{co}}\right)_i - \overline{\left(\frac{f_{cc}}{f_{co}}\right)}\right)^2 \sum_{i=1}^{N}\left(\widetilde{\left(\frac{f_{cc}}{f_{co}}\right)}_i - \overline{\widetilde{\left(\frac{f_{cc}}{f_{co}}\right)}}\right)^2}} \quad (1)$$

$$MAPE = \frac{100}{N}\left(\frac{\sum_{i=1}^{N}\left|\left(\frac{f_{cc}}{f_{co}}\right)_i - \widetilde{\left(\frac{f_{cc}}{f_{co}}\right)}_i\right|}{\sum_{i=1}^{N}\left|\left(\frac{f_{cc}}{f_{co}}\right)_i\right|}\right) \quad (2)$$

Where N is the total number of specimens in each set of SRP and SRG confined concrete columns, $\left(\frac{f_{cc}}{f_{co}}\right)_i$ and $\widetilde{\left(\frac{f_{cc}}{f_{co}}\right)}_i$ are respectively the measured and predicted relative compressive strength for each specimen i, and $\overline{\left(\frac{f_{cc}}{f_{co}}\right)}$ and $\overline{\widetilde{\left(\frac{f_{cc}}{f_{co}}\right)}}$ are their corresponding averages.

Table 4 reported the R and MAPE values for the selected relative compressive strength of SRP and SRG-confined concrete column models. To compare the performance of selected SRP and SRG models in more detail, the measured vs. predicted values of relative compressive strength obtained from SRP and SRG models, as well as the limits of ±3 times of standard deviation (±3 σ), are illustrated in Figs. 3 and 4, respectively. Moreover, Figs. 5 and 6 respectively demonstrated the absolute error values in selected SRP and SRG models for each individual specimen. The ratios of measured to predicted relative compressive strength in selected SRP and SRG models for each tested specimen are provided in Figs. 7 and 8, respectively.

Table 4. The R and MAPE values of selected SRP and SRG models.

Confinement Composite	Model	R	MAPE (%)
SRP	SRP_M1	0.7671	7.39
	SRP_M2	0.7666	10.30
	SRP_M3	0.4431	3.04
	SRP_M4	0.4431	5.55
	SRP_M5	0.4431	6.77
	SRP_M6	0.4431	11.59
SRG	SRG_M1	0.4405	18.45
	SRG_M2	0.3889	19.54
	SRG_M3	0.2899	11.28
	SRG_M4	0.2899	15.90
	SRG_M5	0.2899	17.52
	SRG_M6	0.2899	19.89

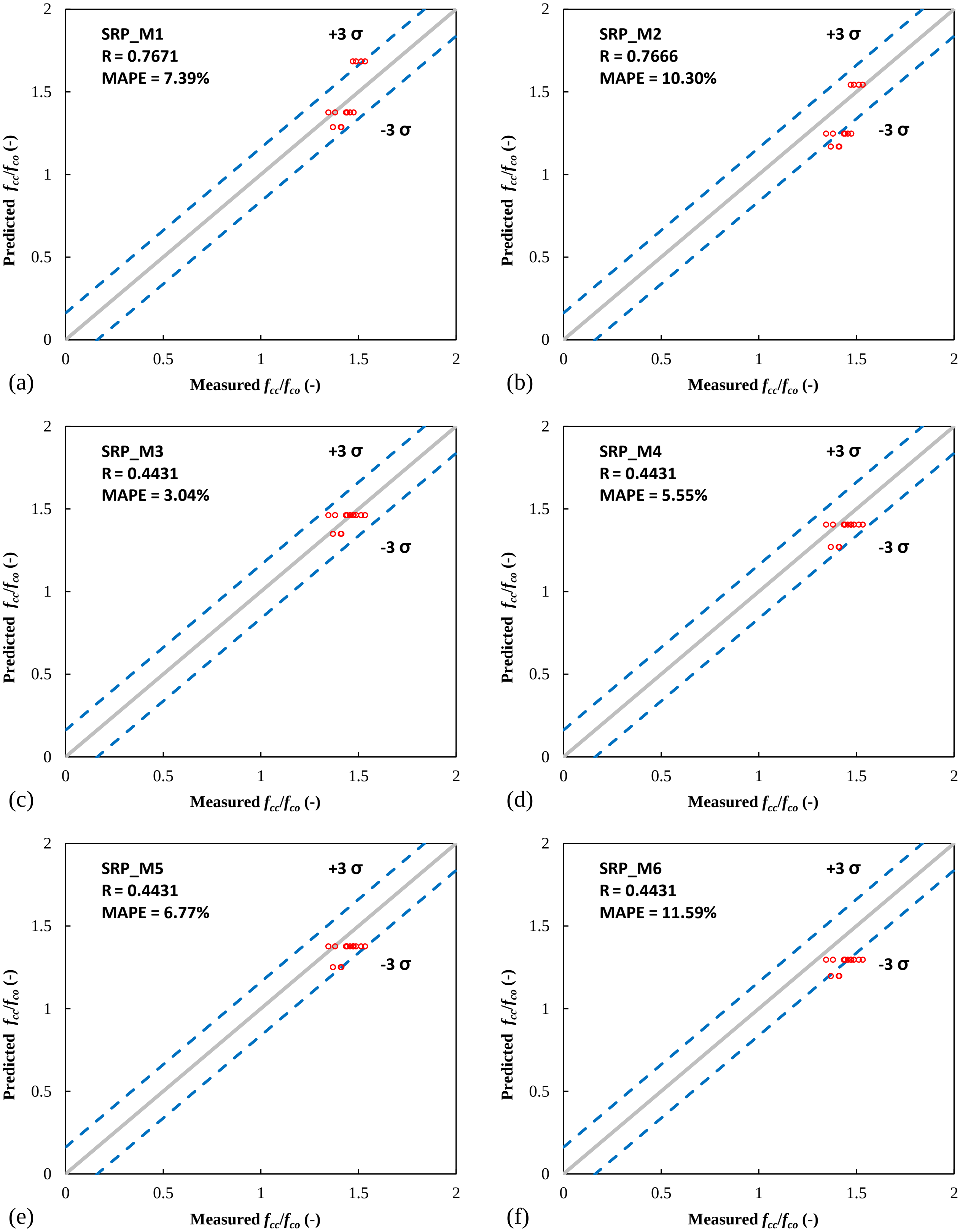

Fig. 3. The measured vs. predicted values of relative compressive strength in selected SRP models: a) SRP_M1; b) SRP_M2; c) SRP_M3; d) SRP_M4; e) SRP_M5 and f) SRP_M6.

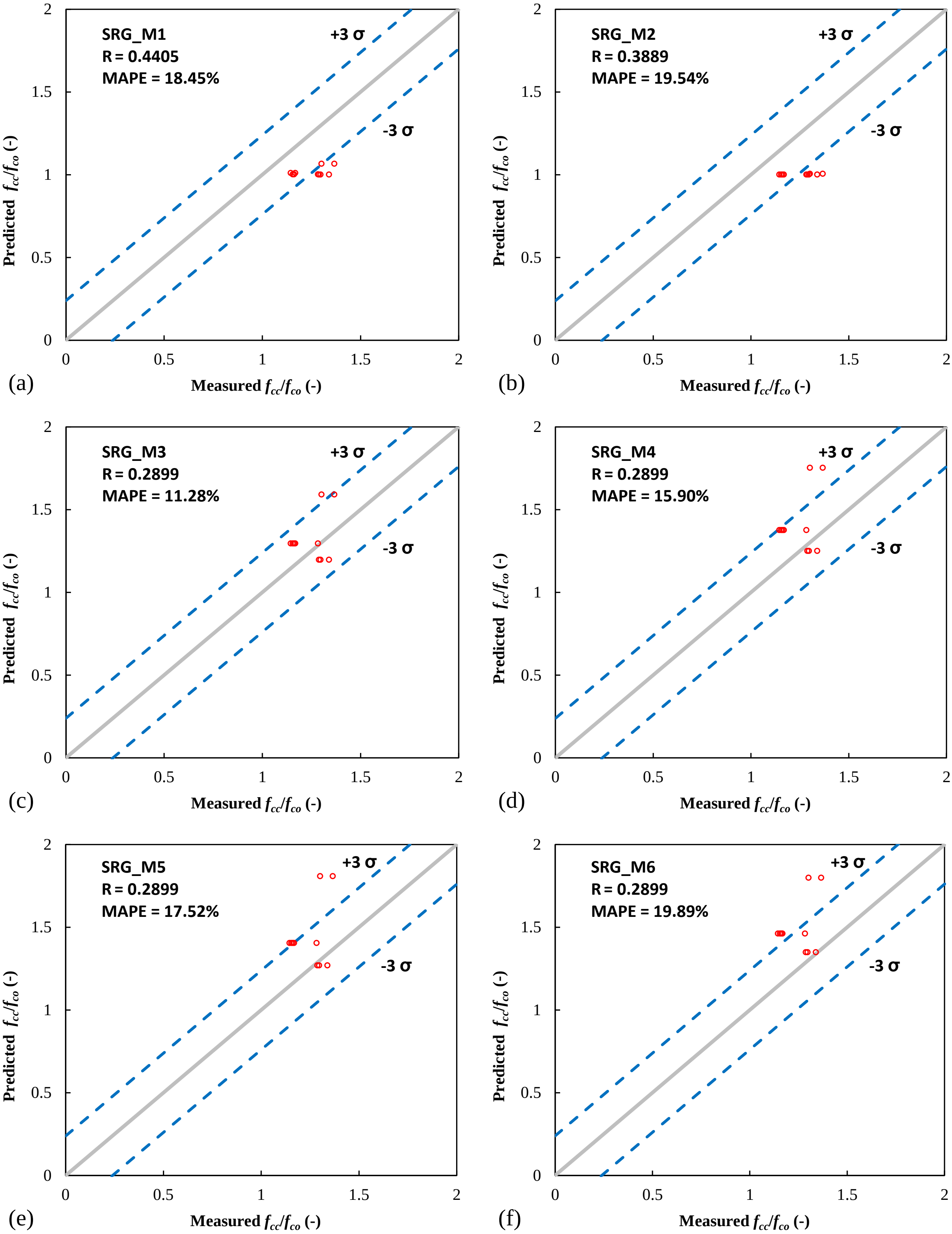

Fig. 4. The measured vs. predicted values of relative compressive strength in selected SRG models: a) SRG_M1; b) SRG_M2; c) SRG_M3; d) SRG_M4; e) SRG_M5 and f) SRG_M6.

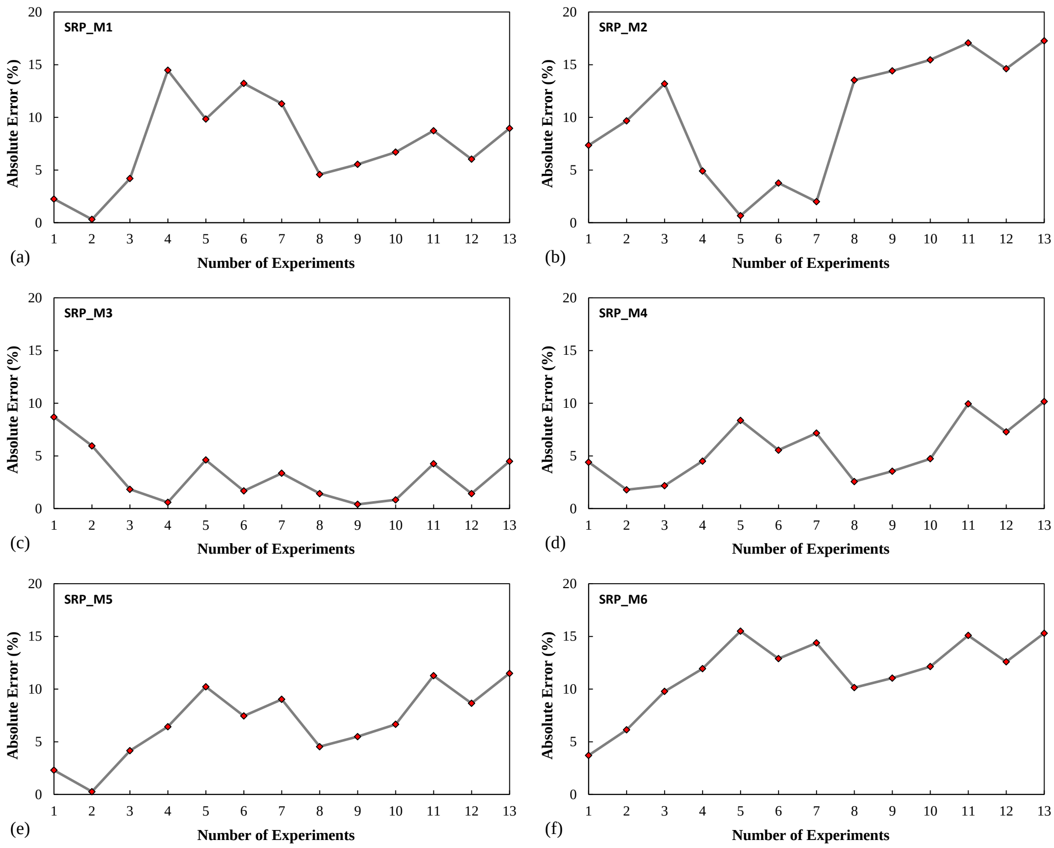

Fig. 5. The absolute error values of relative compressive strength in selected SRP models: a) SRP_M1; b) SRP_M2; c) SRP_M3; d) SRP_M4; e) SRP_M5 and f) SRP_M6.

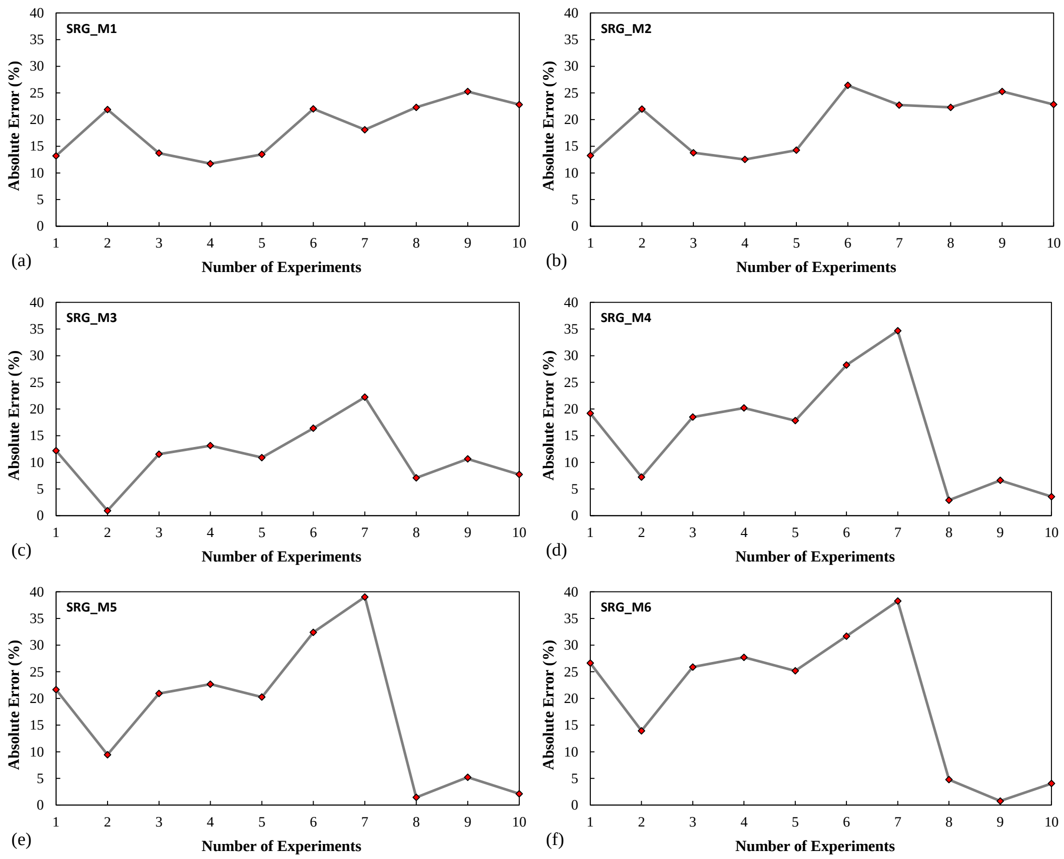

Fig. 6. The absolute error values of relative compressive strength in selected SRG models: a) SRG_M1; b) SRG_M2; c) SRG_M3; d) SRG_M4; e) SRG_M5 and f) SRG_M6.

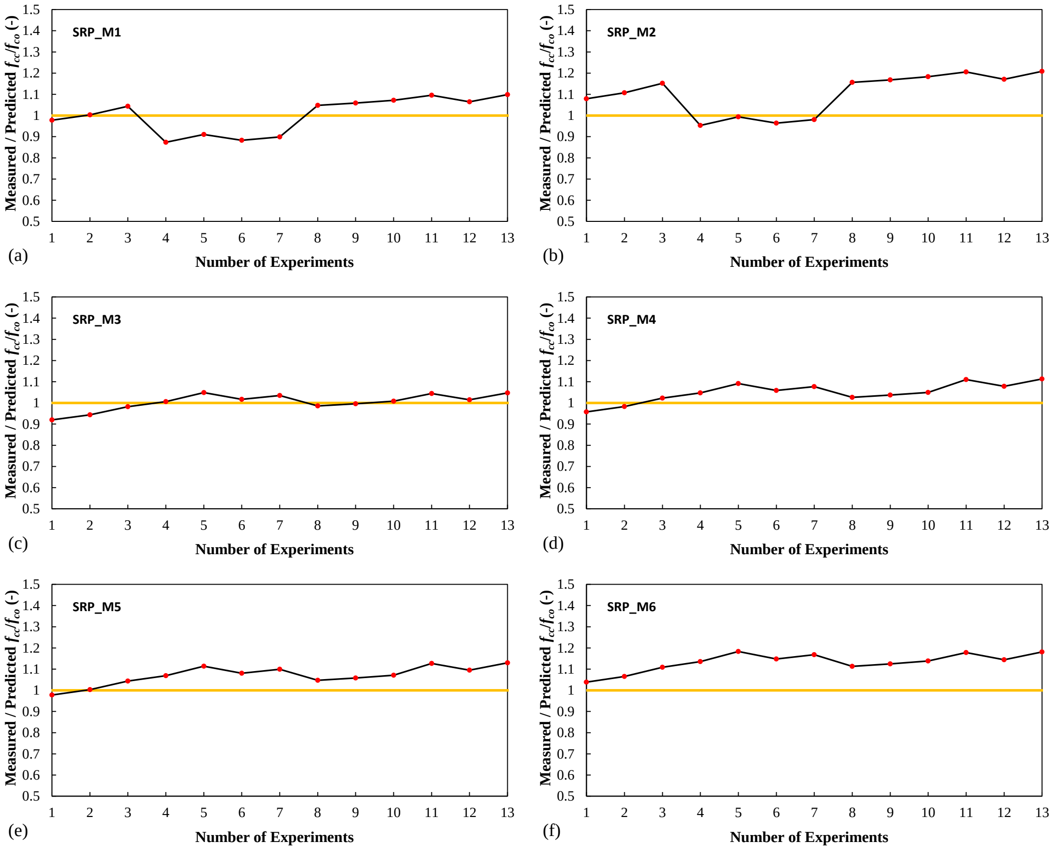

Fig. 7. The ratio of measured to predicted values of relative compressive strength in selected SRP models: a) SRP_M1; b) SRP_M2; c) SRP_M3; d) SRP_M4; e) SRP_M5 and f) SRP_M6.

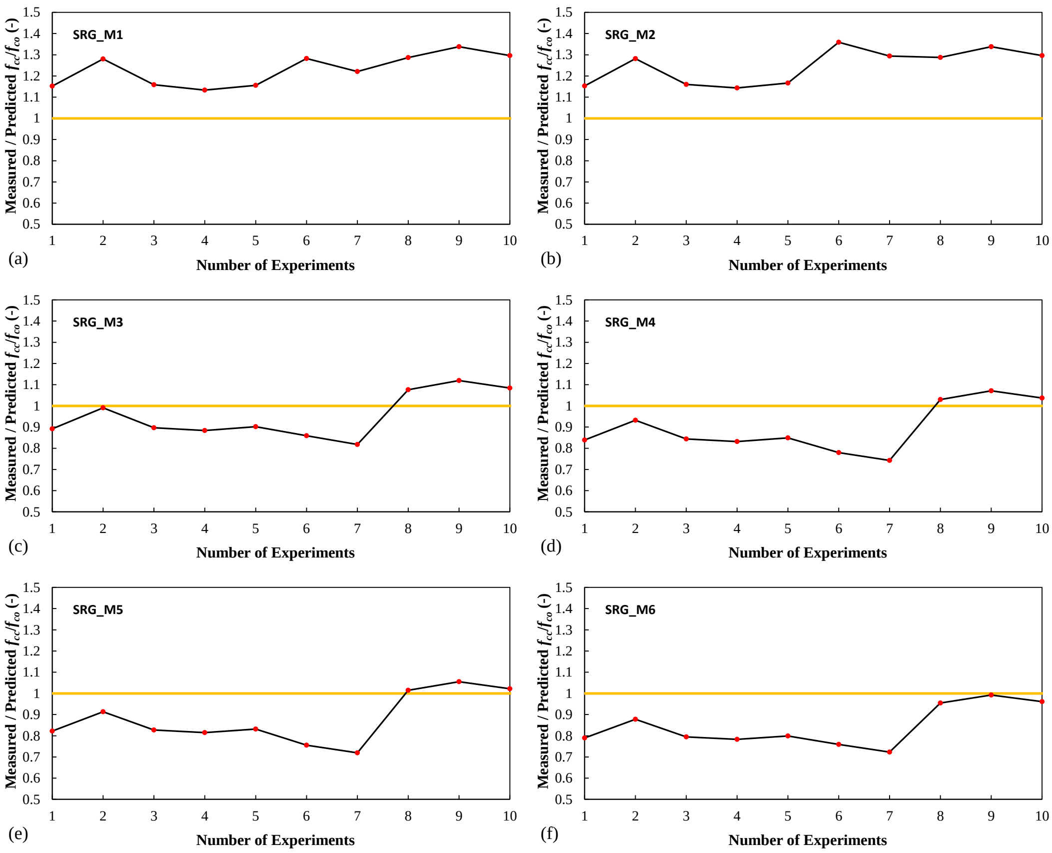

Fig. 8. The ratio of measured to predicted values of relative compressive strength in selected SRG models: a) SRG_M1; b) SRG_M2; c) SRG_M3; d) SRG_M4; e) SRG_M5 and f) SRG_M6.

The presented results in Table 4 and Figs. 3 to 8 showed that for the SRP-confined concrete columns with square cross-sections, the selected model from the CNR-DT200 standard [31] (SRP_M1) with respectively R and MAPE values of 0.7671 and 7.39% outperformed other selected SRP models. Considering just the MAPE error values, the suggested model in the research of Frangou et al. [33] (SRP_M3) with respectively R and MAPE values of 0.4431 and 3.04% has the lowest error values. On the other hand, for the SRG-confined concrete columns with square cross-sections, the selected model from the research work of Isleem et al. [38] (SRG_M1) with respectively R and MAPE values of 0.4405 and 18.45% surpassed the other selected SRP models. Moreover, the results of the presented model in the study of Hoshikuma et al. [34] (SRG_M3) with respectively R and MAPE values of 0.2889 and 11.28% illustrated the lowest error values among other selected SRG models.

As an overall comparison, the results of Table 4 and Figs. 3 to 8 revealed that all the selected SRP models outperformed the selected SRG models. This difference in performance between the selected SRP and SRG models is because most of the proposed models to estimate the relative compressive strength of confined concrete columns were suggested for the fiber-reinforced polymer (FRP) composites rather than the textile-reinforced mortar (TRM) or fiber-reinforced grout (FRG) composites.

6. Conclusion

In this paper, the performance of existing models provided previously to predict the relative compressive strength of concrete columns confined by externally bonded composites was investigated. To achieve this goal, an experimental database including 13 SRP and 10 SRG-confined concrete columns with square cross-sections was compiled and after conducting a trial and error process, six models for SRP and six models for SRG-confined concrete columns were selected. The performance of selected models was evaluated by calculating the Pearson correlation coefficient (R) and the mean absolute percentage error (MAPE) criteria for each selected model. The outcomes of the current study were categorized and summarized below:

- The results showed that for the SRP-confined concrete columns with square cross-sections, the selected model from the CNR-DT200 standard [31] with respectively R and MAPE values of 0.7671 and 7.39% outperformed other selected SRP models. On the other hand, considering just the MAPE error values, the suggested model in the research of Frangou et al. [33] with respectively R and MAPE values of 0.4431 and 3.04% has the lowest error values.
- For the SRG-confined concrete columns with square cross-sections, the selected model from the research work of Isleem et al. [38] with respectively R and MAPE values of 0.4405 and 18.45% surpassed the other selected SRP models. Moreover, the results of the presented model in the study of Hoshikuma et al. [34] with respectively R and MAPE values of 0.2889 and 11.28% illustrated the lowest error values among other selected SRG models.
- As an overall comparison, the results revealed that all the selected SRP models outperformed the selected SRG models. This difference in performance between the selected SRP and SRG models is because most of the proposed models to estimate the relative compressive strength of confined concrete columns were suggested for

the fiber-reinforced polymer (FRP) composites rather than the textile-reinforced mortar (TRM) or fiber-reinforced grout (FRG) composites.

References

[1] Peng X, Yang Q. Damage detection in beam-like structures using static shear energy redistribution. Frontiers of Structural and Civil Engineering 2023. https://doi.org/10.1007/s11709-022-0903-4.

[2] Soleymani A, Saffari H. Seismic Improvement and Rehabilitation of Steel Concentric Braced Frames: A Framework-Based Review. Rehabilitation in Civil Engineering 2023;11:1–23. https://doi.org/10.22075/JRCE.2022.26179.1611.

[3] Soleymani A, Esfahani MR. Effect of concrete strength and thickness of flat slab on preventing of progressive collapse caused by elimination of an internal column. Journal of Structural and Construction Engineering 2019;6:24–40. https://doi.org/10.22065/JSCE.2017.98444.1335.

[4] Shwetha K, Mahesh Kumar C, Dalawai VN, Anadinni S, Sowjanya G. Comparative study on strengthening of concrete using granite waste. Materials Today: Proceedings 2022. https://doi.org/10.1016/j.matpr.2022.03.389.

[5] Pecce M, Ceroni F, Prota A, Manfredi G. Response Prediction of RC Beams Externally Bonded with Steel-Reinforced Polymers. Journal of Composites for Construction 2006;10:195–203. https://doi.org/10.1061/(ASCE)1090-0268(2006)10:3(195).

[6] Onyelowe KC, Jayabalan J, Ebid AM, Samui P, Singh RP, Soleymani A, et al. Evaluation of the Compressive Strength of CFRP-Wrapped Circular Concrete Columns Using Artificial Intelligence Techniques. Designs 2022;6:112. https://doi.org/10.3390/designs6060112.

[7] Dalalbashi A, Ghiassi B, Oliveira D V., Freitas A. Effect of test setup on the fiber-to-mortar pull-out response in TRM composites: Experimental and analytical modeling. Composites Part B: Engineering 2018;143:250–68. https://doi.org/10.1016/j.compositesb.2018.02.010.

[8] Jahangir H, Nikkhah Z, Rezazadeh Eidgahee D, Esfahani MR. Performance Based Review and Fine-Tuning of TRM-Concrete Bond Strength Existing Models. Soft Computing in Civil Engineering 2023;7:43–55. https://doi.org/10.22115/SCCE.2022.349483.1476.

[9] Carozzi FG, Poggi C, Bertolesi E, Milani G. Ancient masonry arches and vaults strengthened with TRM, SRG and FRP composites: Experimental evaluation. Composite Structures 2018;187:466–80. https://doi.org/10.1016/j.compstruct.2017.12.075.

[10] Nematzadeh M, Mousavimehr M, Shayanfar J, Omidalizadeh M. Eccentric compressive behavior of steel fiber-reinforced RC columns strengthened with CFRP wraps: Experimental investigation and analytical modeling. Engineering Structures 2021;226:111389. https://doi.org/10.1016/J.ENGSTRUCT.2020.111389.

[11] Pan JL, Xu T, Hu ZJ. Experimental investigation of load carrying capacity of the slender reinforced concrete columns wrapped with FRP. Construction and Building Materials 2007;21:1991–6. https://doi.org/10.1016/J.CONBUILDMAT.2006.05.050.

[12] Al-Nimry H, Neqresh M. Confinement effects of unidirectional CFRP sheets on axial and bending capacities of square RC columns. Engineering Structures 2019;196:109329. https://doi.org/10.1016/J.ENGSTRUCT.2019.109329.

[13] Ghorbel E, Limaiem M, Wardeh G. Mechanical performance of bio-based FRP-confined recycled aggregate concrete under uniaxial compression. Materials 2021;14. https://doi.org/10.3390/ma14071778.

[14] Yan Z, Pantelides CP, Reaveley LD. Fiber-reinforced polymer jacketed and shape-modified compression members: I - Experimental behavior. ACI Structural Journal 2006;103:885–93.

[15] Triantafillou TC., Papanicolaou CG., Zissimopoulos P., Laourdekis T. Concrete confinement with textile-reinforced mortar

jackets. ACI Structural Journal 2006;103:28–37.

[16] Zhou JKK, Lin G, Teng JGG. Stress-strain behavior of FRP-confined concrete containing recycled concrete lumps. Construction and Building Materials 2021;267:120915. https://doi.org/10.1016/j.conbuildmat.2020.120915.

[17] Ozbakkaloglu T, Lim JC. Axial compressive behavior of FRP-confined concrete: Experimental test database and a new design-oriented model. Composites Part B: Engineering 2013;55:607–34. https://doi.org/10.1016/j.compositesb.2013.07.025.

[18] Chotickai P, Tongya P, Jantharaksa S. Performance of corroded rectangular RC columns strengthened with CFRP composite under eccentric loading. Construction and Building Materials 2021;268:121134. https://doi.org/10.1016/J.CONBUILDMAT.2020.121134.

[19] Sadeghian P, Fam A. Improved design-oriented confinement models for FRP-wrapped concrete cylinders based on statistical analyses. Engineering Structures 2015;87:162–82. https://doi.org/10.1016/j.engstruct.2015.01.024.

[20] Han Q, Yuan WY, Ozbakkaloglu T, Bai YL, Du XL. Compressive behavior for recycled aggregate concrete confined with recycled polyethylene naphthalate/terephthalate composites. Construction and Building Materials 2020;261:120498. https://doi.org/10.1016/j.conbuildmat.2020.120498.

[21] Lam L, Teng JG. Design-Oriented Stress-Strain Model for FRP-Confined Concrete in Rectangular Columns. Journal of Reinforced Plastics and Composites 2003;22:1149–86. https://doi.org/10.1177/0731684403035429.

[22] Triantafillou TC, Papanicolaou CG, Zissimopoulos P, Laourdekis T. Concrete confinement with textile-reinforced mortar jackets. ACI Structural Journal 2006;103:28–37. https://doi.org/10.14359/15083.

[23] Yin HY, Xun Y, Ji C Bin, Sun S. Experimental Investigation of Concrete Confinement with Textile Reinforced Concrete. Applied Mechanics and Materials 2015;752–753:702–10. https://doi.org/10.4028/www.scientific.net/amm.752-753.702.

[24] Binici B. Design of FRPs in circular bridge column retrofits for ductility enhancement. Engineering Structures 2008;30:766–76. https://doi.org/10.1016/j.engstruct.2007.05.012.

[25] Harajli MH. Axial stress–strain relationship for FRP confined circular and rectangular concrete columns. Cement and Concrete Composites 2006;28:938–48. https://doi.org/10.1016/J.CEMCONCOMP.2006.07.005.

[26] Faustino P, Chastre C. Analysis of load–strain models for RC square columns confined with CFRP. Composites Part B: Engineering 2015;74:23–41. https://doi.org/10.1016/j.compositesb.2015.01.002.

[27] J. ZJ, G. TJ, Guan L, J. LL. Large-Scale FRP-Confined Rectangular RC Columns with Section Curvilinearization under Axial Compression. Journal of Composites for Construction 2021;25:4021020. https://doi.org/10.1061/(ASCE)CC.1943-5614.0001129.

[28] Mohebi B, Hosseinifard SM, Bastami M. Plastic hinge characteristics of RC rectangular columns with Fiber Reinforced Polymer (FRP). Computers and Concrete 2016;18:853–76. https://doi.org/https://doi.org/10.12989/cac.2016.18.4.853.

[29] Jahangir H, Soleymani A, Esfahani MR. Investigating the Confining Effect of Steel Reinforced Polymer and Grout Composites on Compressive Behavior of Square Concrete Columns. Iranian Journal of Science and Technology, Transactions of Civil Engineering 2023;47:775–91. https://doi.org/10.1007/s40996-022-00917-7.

[30] Pimanmas A, Saleem S. Evaluation of Existing Stress–Strain Models and Modeling of PET FRP–Confined Concrete. Journal of Materials in Civil Engineering 2019;31:04019303. https://doi.org/10.1061/(ASCE)MT.1943-5533.0002941.

[31] CNR-DT200. Guide for the design and construction of externally bonded FRP systems for strengthening existing structures. 2004.

[32] Colajanni P, De Domenico F, Recupero A, Spinella N. Concrete columns confined with fibre reinforced cementitious mortars: Experimentation and modelling. Construction and Building Materials 2014;52:375–84. https://doi.org/10.1016/j.conbuildmat.2013.11.048.

[33] Frangou M, Pilakoutas K, Dritsos S. Structural repair/strengthening of RC columns. Construction and Building Materials 1995;9:259–66. https://doi.org/10.1016/0950-0618(95)00013-6.

[34] Hoshikuma J, Kawashima K, Nagaya K, Taylor AW. Stress-Strain Model for Confined Reinforced Concrete in Bridge Piers. Journal of Structural Engineering 1997;123:624–33. https://doi.org/10.1061/(ASCE)0733-9445(1997)123:5(624).

[35] Thériault M, Neale KW. Design equations for axially loaded reinforced concrete columns strengthened with fibre reinforced polymer wraps. Canadian Journal of Civil Engineering 2000;27:1011–20. https://doi.org/10.1139/l00-019.

[36] Kumutha R, Vaidyanathan R, Palanichamy MS. Behaviour of reinforced concrete rectangular columns strengthened using GFRP. Cement and Concrete Composites 2007;29:609–15. https://doi.org/10.1016/j.cemconcomp.2007.03.009.

[37] Islam MM, Choudhury MSI, Amin AFMS. Dilation Effects in FRP-Confined Square Concrete Columns Using Stone, Brick, and Recycled Coarse Aggregates. Journal of Composites for Construction 2016;20:04015017. https://doi.org/10.1061/(ASCE)CC.1943-5614.0000574.

[38] Isleem HF, Wang Z, Wang D. A new model for reinforced concrete columns strengthened with fibre-reinforced polymer. Proceedings of the Institution of Civil Engineers: Structures and Buildings 2020;173:602–22. https://doi.org/10.1680/jstbu.18.00159.